EUROPEAN ORGANIZATION FOR NUCLEAR RESEARCH

CERN/PS/85-1 (AA)

THE CERN ANTIPROTON COLLECTOR

B. Autin

(Lecture given to the CERN Accelerator School,
Course on Antiprotons for Colliding Beam Facilities,
11-21 October 1983).

Geneva, Switzerland
January 1985

?HE CERN ANTIPROTON COLLECTOR*)

?. Autin
?ERN, Geneva, Switzerland

ABSTRACT

The Antiproton Collector is a new ring of much larger acceptance than the present accumulator. It is designed to receive 10^8 antiprotons per PS cycle. In order to be compatible with the Antiproton Accumulator, the momentum spread and the emittances are reduced from 6% to 0.2% and from 200 π mm·mrad to 25 π mm·mrad respectively. In addition to the ring itself, the new target area and the modifications to the stochastic systems of the Antiproton Accumulator are described.

INTRODUCTION

It is not the first time that I present the design of the Antiproton Collector (ACOL)[1-5], but I must confess that, today, I have the feeling of a climber at the foot of a mountain, a blend of emotion and enthusiasm that I shall try to convey to you. I shall limit myself to a strict technical description of the aspects specific to the project. Topics such as civil and mechanical engineering, radiation shielding, vacuum, geometrical survey, instrumentation, or controls are of fundamental importance but common to all accelerators and will not be treated here. Further information can be found in the design report[6].

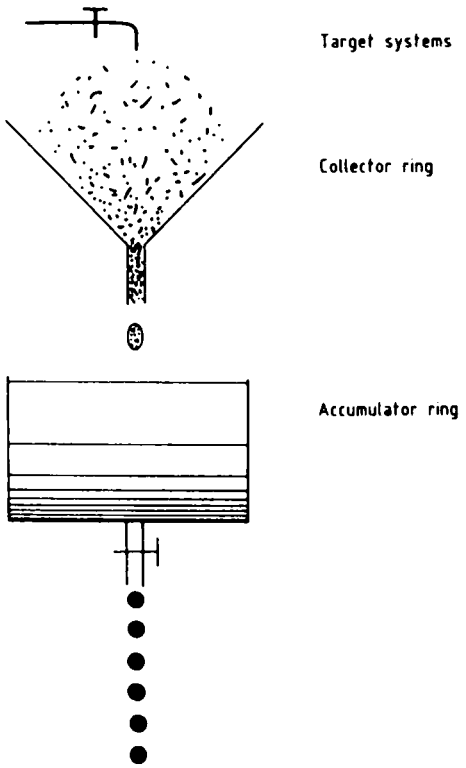

Fig. 1
Hydraulic analogy of an antiproton source

*) The written version of this talk given at the CERN Accelerator School in October 1983 has been produced one year later and incorporates modifications made during 1984. What was a proposal became the ACOL project in January 1984.

Let me explain the term of 'Collector'. Some people speak of 'debunchers' or of 'precoolers'; as the two functions are performed here, a third word was necessary. Moreover, maybe a deeper reason for this name is the analogy of the tap, the funnel, and the reservoir as characterizing the various functions of the antiproton source (Fig. 1) which are similar to those John Peoples has just described for the Tevatron I project[7]; namely antiproton production, collection in a machine of large acceptance, compression of the whole phase-space volume in the same machine and accumulation in a second machine.

In this new version of the CERN antiproton source, the Antiproton Accumulator (AA) ring is the reservoir, the collector surrounds the AA, and exotic focusing systems are implemented in the target area. The realm of antiproton physics evolves so rapidly that the Collector is attractive if it is completed within a short time and therefore physics beams are foreseen in 1987. Last, but not least, such a programme must be met within the normal CERN budget and the need for ingenious and innovative solutions is a real challenge.

2. PARTICLE PRODUCTION

Up to the summer of 1983, the AA received typically six million antiprotons per pulse. With the collector, the goal is to capture 10^8 antiprotons per pulse. The factor of 16 is gained by splitting the functions of collection and accumulation between two machines. Compared to the AA, the collector has thus four times the betatron acceptance (200 π mm·mrad) and four times the momentum acceptance (6%). To populate the acceptance at the best efficiency, special devices are required: a pulsed target and high magnetic field gradient lenses to achieve the ultimate proton focusing on the target and the initial antiproton focusing.

2.1 Pulsed target

The principle of a pulsed target is recalled in Fig. 2. It consists of mapping the triangular phase-space diagram at the end of a long and thin target into an ellipse. The

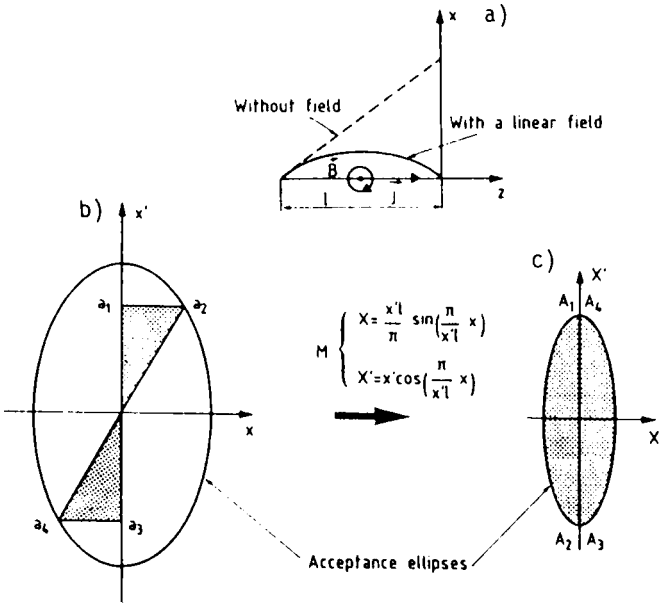

Fig. 2 Phase-space mapping at the end of a thin pulsed target when a particle emitted at the origin undergoes half a sinusoidal oscillation over the target length. (a) Particle trajectories. (b) Phase-space particle distribution without field. (c) Phase-space particle distribution with a linear field.

stronger the current density, the smaller the minor axis of the ellipse and the denser the transverse phase space. A real target has a finite thickness; antiprotons are reabsorbed partially inside the target and the primary protons get defocused. Because of these limitations, the antiprotons undergo half a sine period only over the target length. Typical currents of the order of 250 kA in a 3 mm diameter copper rod pulsed in a few microseconds are contemplated. Improvements in the antiproton-yield have already been observed at a lower current density[8]. Technological problems need to be solved to improve the reliability.

2.2 High magnetic field gradient lenses

At the end of the target, the phase-space ellipse is upright and elongated along the angle axis. The area of the antiproton spot size is 30 mm^2 and the beam divergence about 70 mrad. Conventional iron quadrupoles cannot focus high-energy beams of so wide a divergence and a special intermediate lens is required. Two types of lenses are at present being developed in parallel: one is a fully solid structure whose active part is a lithium rod (Fig. 3), the other uses a plasma column as a focusing medium (Fig. 4). The reabsorption of

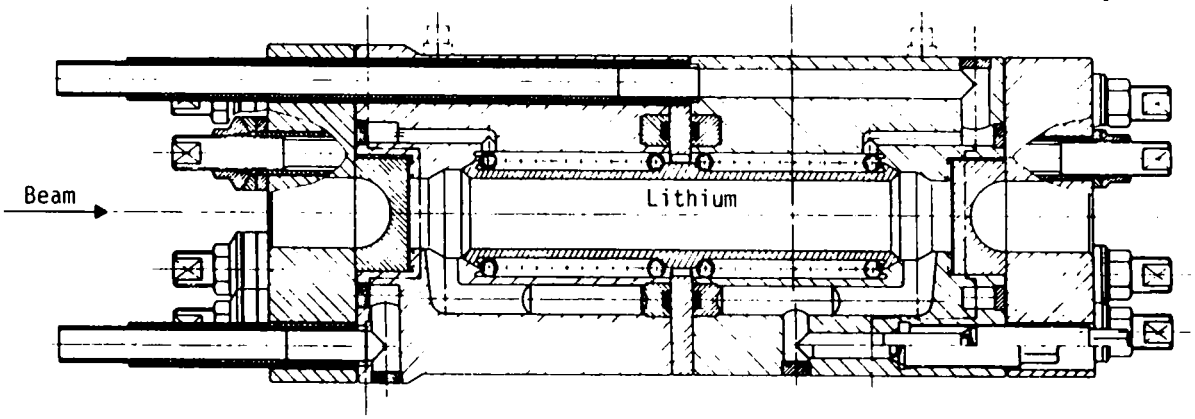

Fig. 3 Lithium lens

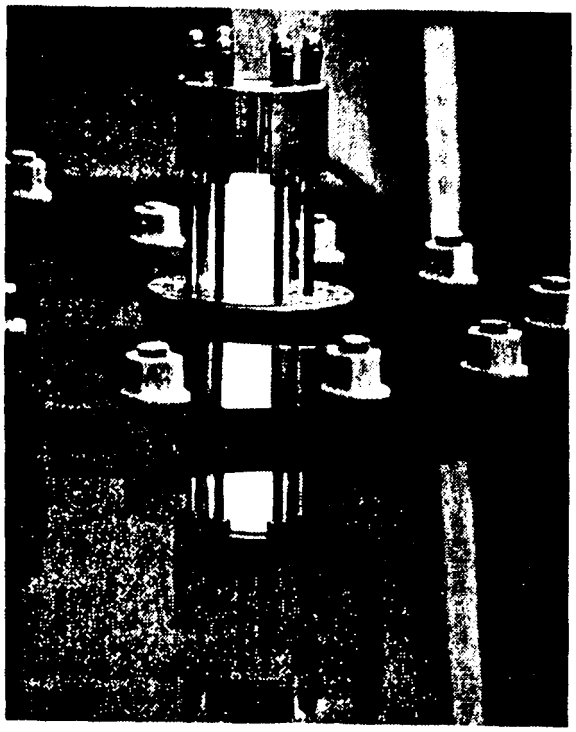

Fig. 4
Plasma lens prototype

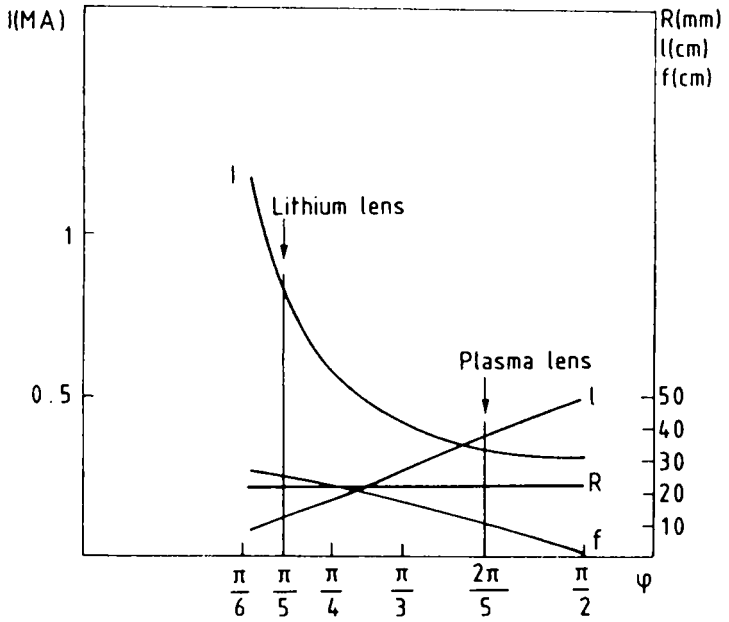

Fig. 5 Characteristics of a large-aperture axisymmetric lens: ℓ = length. R = radius. f = distance to the target. I = current. The parameter of comparison is the phase ϕ of the transverse oscillation of the particle in the linear field of the lens.

antiprotons is negligible for a plasma but limits the length of a lithium lens. The two lenses have thus two different regimes of operation (Fig. 5). Furthermore, the current penetrates the lithium in 1.5 ms, whereas the 'Z-pinch' takes place in a few microseconds for a plasma lens of the same diameter (4 cm). The final choice will be based on the respective reliability, performance, and cost of these devices.

3. BEAM TRANSFERS

The two main reasons that have determined the implementation of the collector in the AA hall are the saving of major civil engineering and the use of existing transfer lines. However, the tight space constraints have imposed special solutions. In order to make the hall radiation proof, it is envisaged to reduce the momentum acceptance of the injection line by adding extra spectrometer magnets. Where the injected beam enters the collector, the yoke and the coils of a main bending magnet are modified to leave space for the injection pipe, and three combined-function magnets have the structure of half quadrupoles closed on one side by a neutral pole. The septum magnet is pulsed and the full aperture kicker has a travelling wave structure. In the transfer from the collector to the accumulator the orbit dispersion is not matched; this simplification is justified because the beam momentum spread at the exit from the collector is small. The extraction from the AA towards the loop which returns to the PS is three dimensional. Since the collector and the accumulator lie in the same plane, the extraction channel plunges below the collector just after the ejection which takes place in the horizontal plane.

4. LATTICE

4.1 Optics

The lattice is made of 28 FODO cells. The focusing is strong and the dispersion in revolution frequencies is positive. The ring structure is that of a square elongated on

two opposite sides (Fig. 6). The straight sections DA, A'B', BC, and C'D' have no orbit dispersion, whereas sections Aα, α'A', B'β', βB, Cγ, γ'C', and D'δ' have a quasi-zero orbit dispersion for they contain combined-function magnets whose bending angle is small. These small bending angles are necessary to satisfy the topology imposed by the accumulator and the various transfer lines.

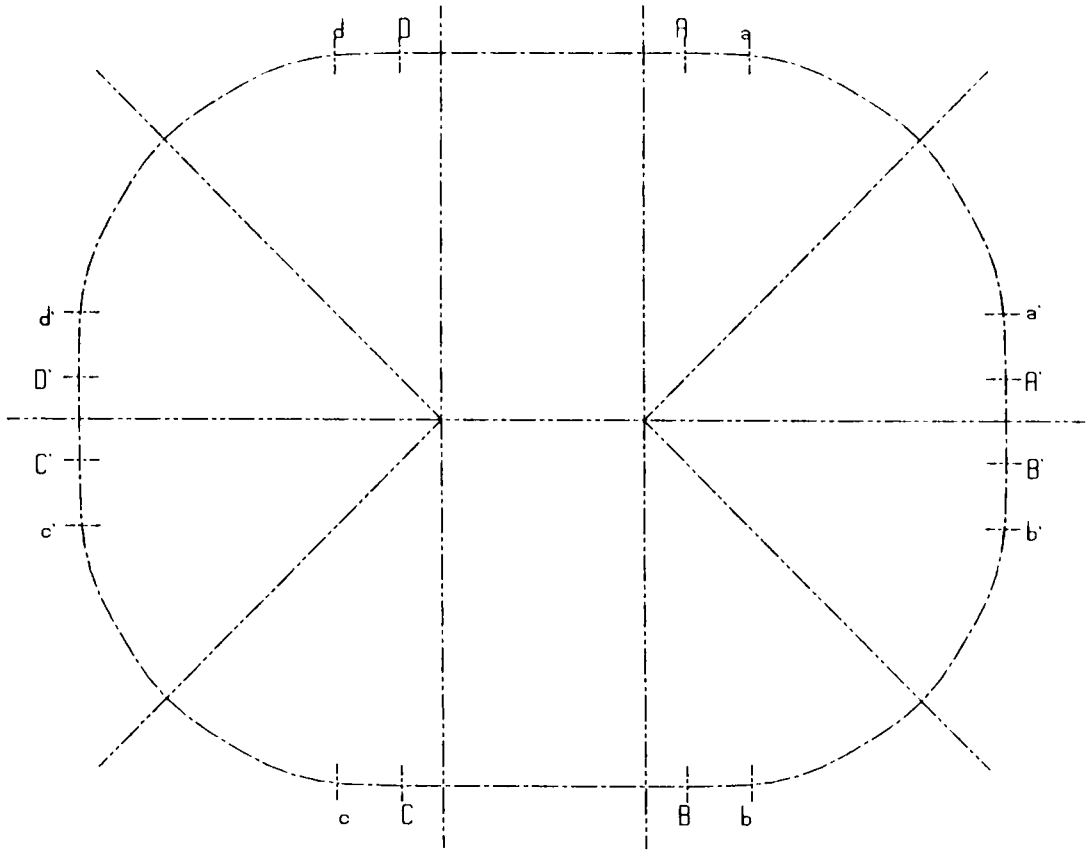

Fig. 6 Ring geometry

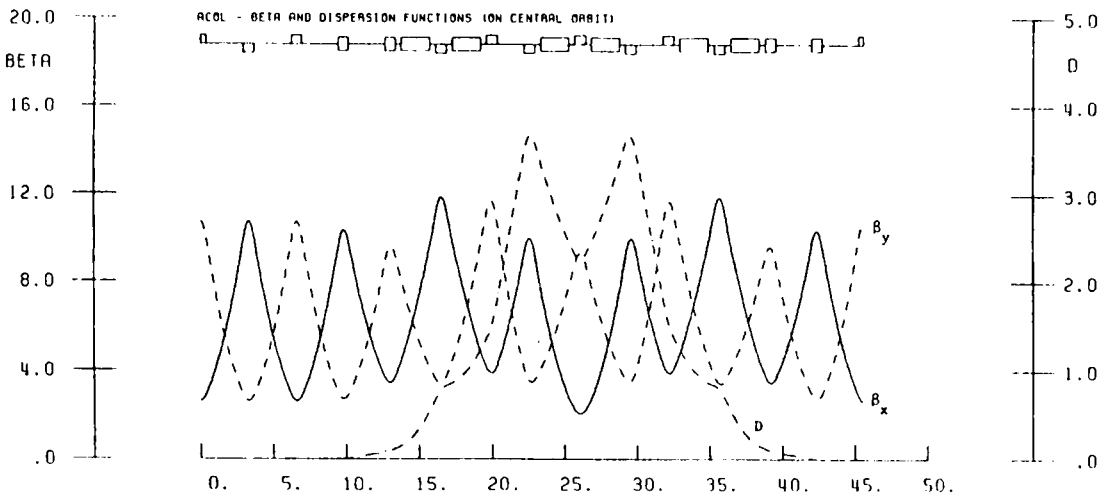

Fig. 7 Characteristic functions of the ACOL lattice

The β and D_x functions are plotted in Fig. 7. The tunes

$$Q_x = 5.465, \quad Q_y = 5.44$$

correspond to the maximum aperture compatible with quadrupole strengths and permit a symmetric disposition of the stochastic cooling pick-ups and kickers about the ring centre. The proximity of half-integer stopbands requires tight tolerances on the gradient errors ($\Delta G/G < 10^{-3}$).

The variations of the tunes (Fig. 8) and of D_x with the momentum in the zero-dispersion sections are controlled by three families of sextupoles. If the situation is the same as in the AA, the reason for controlling D_x is different. In the AA, the beam stays several hours and a transverse blow-up due to synchro-betatron coupling is to be avoided. In ACOL, the beam stays a little more than two seconds and long term effects are not relevant; however, the stochastic cooling is limited by the available radiofrequency power, which must be concentrated in the betatron signal and not dissipated in the longitudinal signal. A consequence of this sextupole scheme is the linear variation of the revolution frequency dispersion η with the particle momentum (Fig. 8). The η variation slightly alters the linearity of the bunch rotation (Section 5), but may be used advantageously for the stochastic cooling (Section 6).

As the beam emittance is large, the stability of large-amplitude oscillations is questionable. Particle tracking has been performed (Fig. 9). The transfer of transverse energy from the horizontal plane to the vertical plane and vice versa seems to be the most harmful effect and may cause the loss of 10% of the particles. As a safety measure, the aperture of the machine is calculated for a 240 π mm·mrad beam emittance. Moreover, a set of two pairs of sextupoles disposed symmetrically with respect to the end of the major axis in zero-dispersion regions improves the dynamic aperture of the machine; in each pair, the sextupoles are $2\pi/3$ distant in betatron phase.

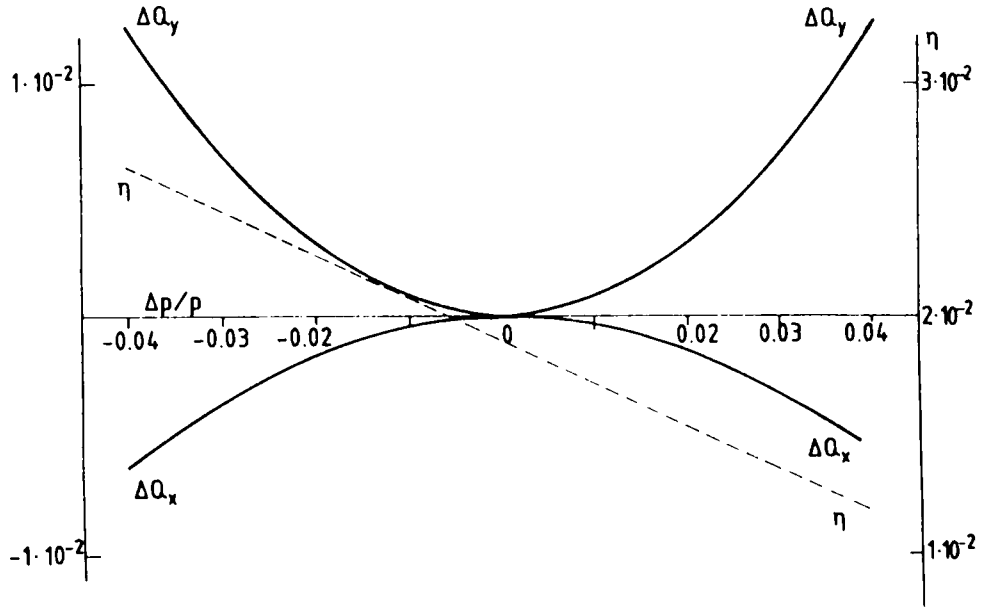

Fig. 8 Chromaticity and η variation in the CERN Antiproton Collector after sextupole corrections.

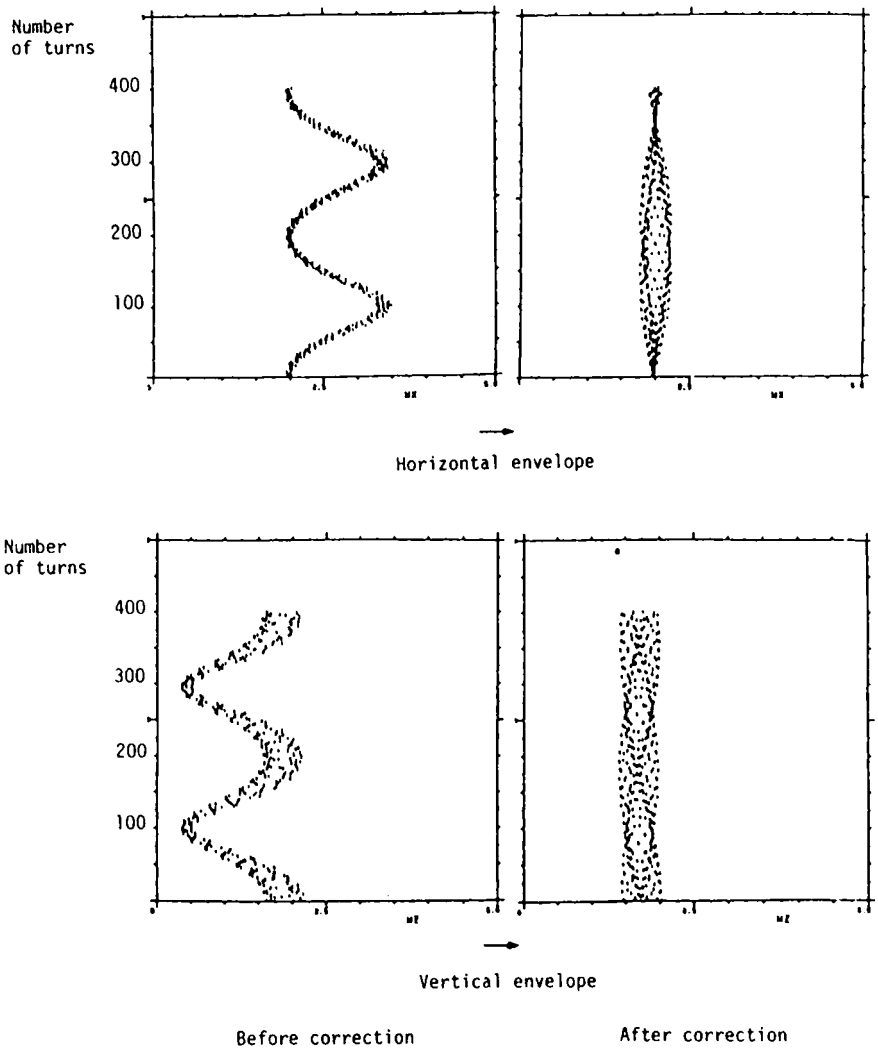

Fig. 9 Beam envelope oscillations in the middle of a long straight section.

4.2 Magnets

Owing to the strong modulation of the beam envelope, the magnets have been shared in families of 'wide' and 'narrow' elements. All the dipoles have the same bending angle; they are of H-type and their coil has a saddle shape (Fig. 10).

The two types of quadrupoles (Fig. 11) differ not only in their transverse dimensions but also in the multipole contents of their profiles. The narrow ones are pure fully symmetric quadrupoles and are located in the zero or quasi-zero dispersion regions. In the arcs, the quadrupoles are wide and sextupole components are combined in their profile. The sextupole component introduces three subfamilies, two in F quadrupoles and one in D quadrupoles, each characterized by a given ratio G'/G, where G is the field gradient and G' its radial derivative:

$$\left.\frac{G'}{G}\right|_{F_1} = 0.6\ m^{-1}, \quad \left.\frac{G'}{G}\right|_{F_2} = 1.4\ m^{-1}, \quad \left.\frac{G'}{G}\right|_{D} = 1.4\ m^{-1}\ .$$

It is not completely fortuitous that the two profiles F_2 and D are identical. The simplification is possible because the control of D_x is sufficiently precise with equal values of G'/G.

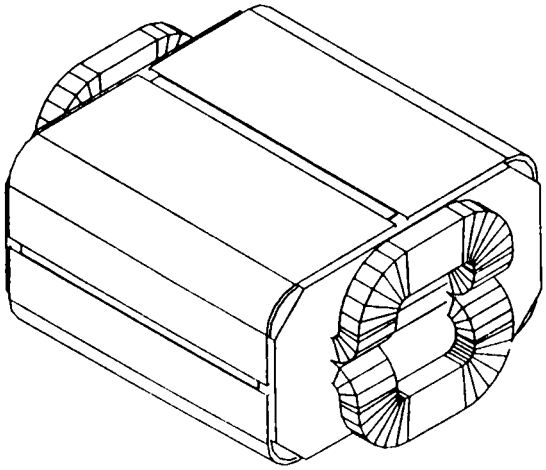

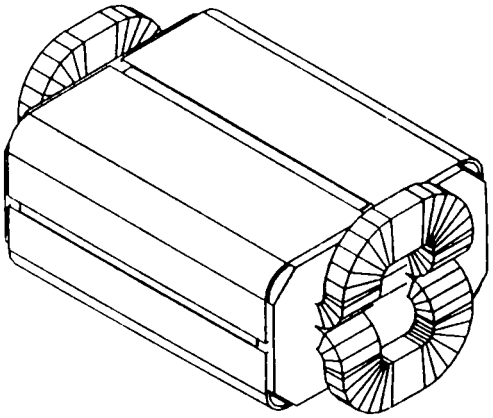

	Wide dipole	Narrow dipole
Pole width (mm)	540	370
Gap height (mm)	114	114
Ampere turns (At)	139320	139320
Field (T)	1.5	1.5
Length (mm)	1836	1836

Fig. 10 ACOL dipoles

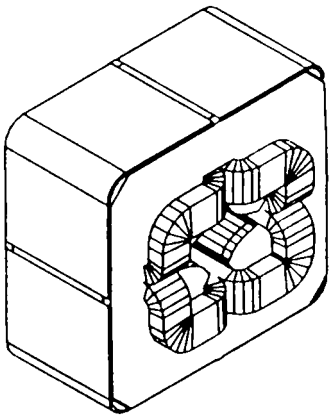

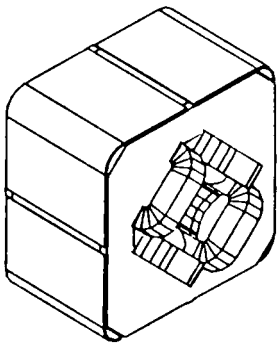

	Wide quadrupole	Narrow quadrupole
Good field width (mm)	340	260
Good field height (mm)	120	120
Max. ampere turns (At)	31280	46930
Max. gradient (T m^{-1})	6.45	6.92
Length (mm)	620	607

Fig. 11 ACOL quadrupoles

The regular modulation of the β function and the matching of the zero-dispersion sections are obtained with seven different gradient strengths. In order to make the operation of the machine easy, the number of turns and the effective lengths are adjusted in each quadrupole family so that all the quadrupoles can be connected in series. Trim currents are available in the wide quadrupoles to vary the betatron tunes and the orbit dispersion independently.

5. DEBUNCHING

It is a matter of common understanding that each time a function can be performed either by a coherent or by a stochastic method, the coherent method is chosen for its rapidity and simplicity. This is precisely the case for the reduction of beam momentum spread which is achieved by 'bunch rotation', 'adiabatic debunching' and, in the last stage only, by stochastic cooling. The first two stages are based on a trade-off of time and momentum spreads; they require an initial short bunch length. The time structure of the antiprotons is the exact replica of the time structure of the primary proton beam.

For the ACOL mode of operation, the protron synchrotron (PS) will use a novel procedure (Fig. 12). Two booster rings are injected into the PS so that they fill half the ring, the

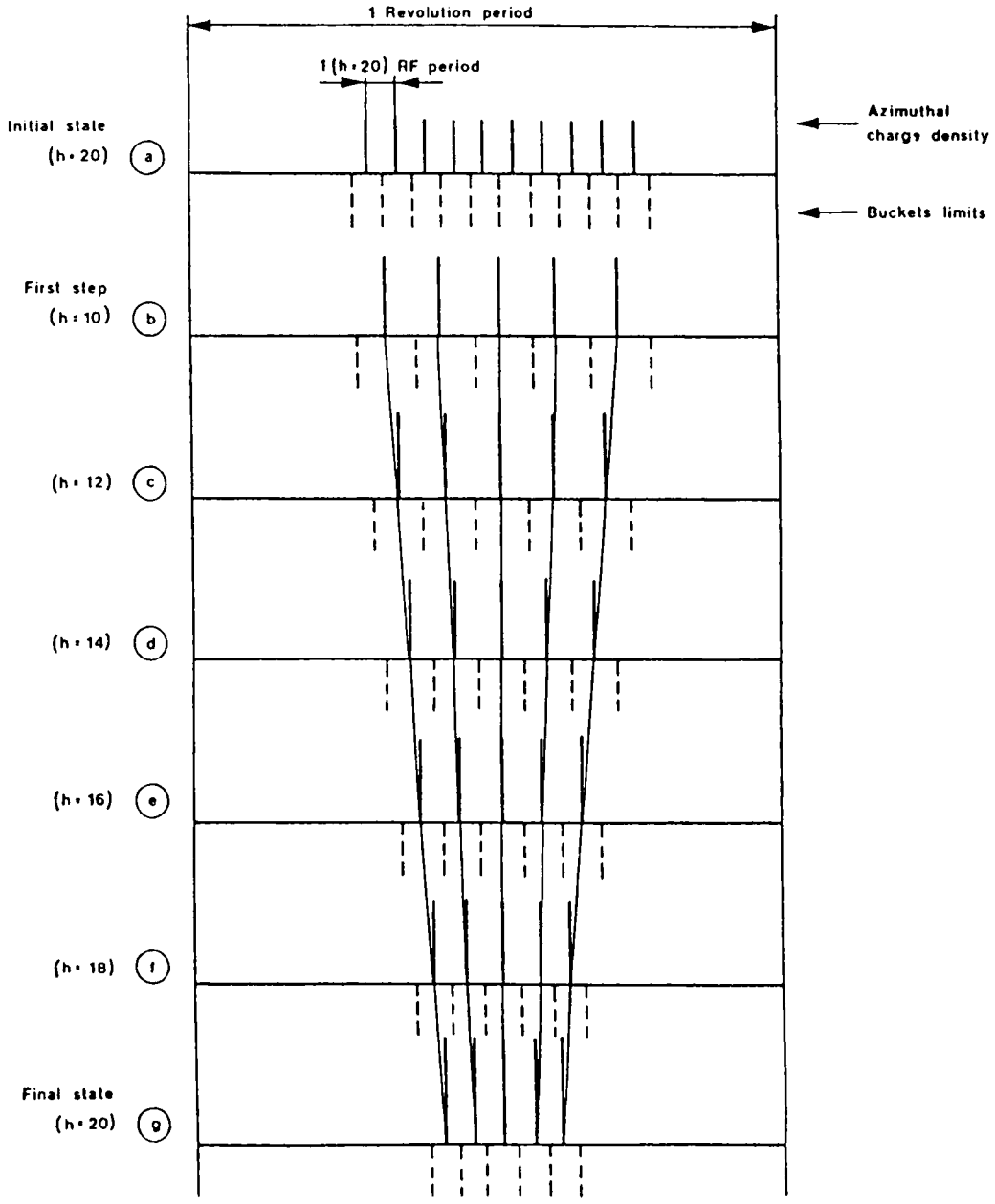

Fig. 12 Coarse description of the azimuthal charge density during the merging process in the Proton Synchrotron.

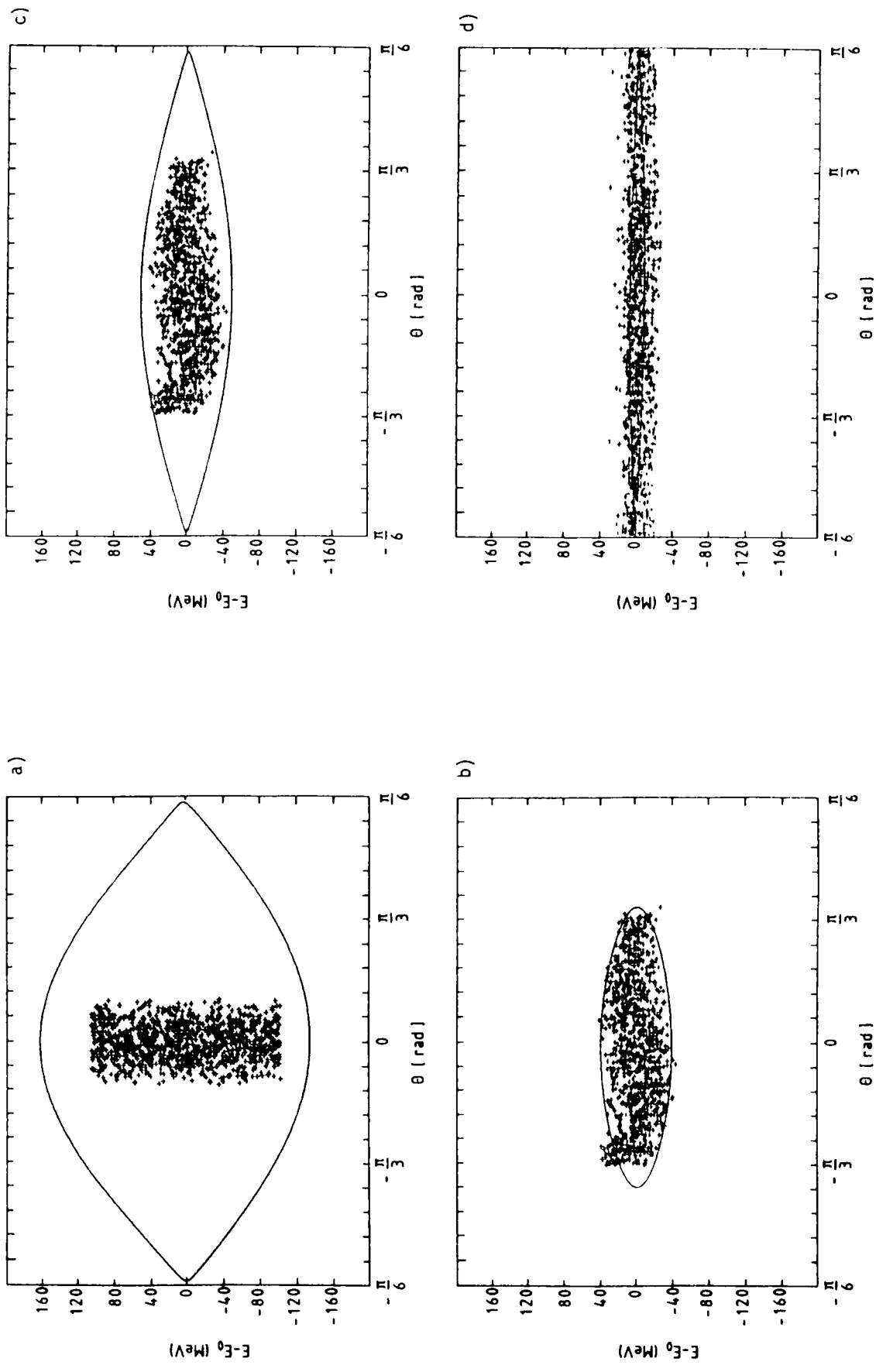

Fig. 13 Debunching in ACOL. (a) Initial configuration of the bunch in the longitudinal phase space. (b) After bunch rotation. (c) At the beginning of the adiabatic debunching. (d) After full debunching.

other half being empty. The bunches are captured on the twentieth harmonic of the revolution frequency. After capture, the radiofrequency (RF) is halved and two consecutive bunches migrate into the same potential well; the beam becomes composed of five instead of the ten initial bunches. The frequency is then raised to its initial value by steps of two harmonics at a time, forcing the bunches to move azimuthally towards the central bunch which is not affected. At the end of the merging process, the five bunches occupy a quarter of the PS ring. The RF gymnastics requires a modest voltage (70 kV) and makes possible the final bunch compression obtained by an abrupt rise of the voltage to its maximum value (200 kV).

Under the effect of this voltage, the bunches which are no longer matched to the RF wave 'rotate' in the longitudinal phase space at the synchrotron frequency; they reach their minimum length ($\sim$ 20 ns) after a quarter period and are ejected towards the target.

In the collector, a reciprocal process occurs (Fig. 13). Just after injection, the antiproton bunches are captured in an RF wave of large amplitude and rotate back towards their maximum length -- and minimum energy spread. After a quarter of synchrotron period, some space remains between the bunches. The voltage is suddenly decreased to match the bunches and adiabatically lowered to complete the debunching.

The assymmetry of the separatrix in Fig. 13 is due to the η variation. This characteristic of the machine, albeit harmful to the linearity of the bunch rotation, is quite tolerable since the final momentum spread is inferior to 1.5%.

The RF cavities are two toroidal 'pillboxes'. They are driven by triode amplifiers of 3 MW peak power delivering a maximum voltage of 0.7 MV in the gap of each cavity.

6. STOCHASTIC COOLING

After debunching, the beam is first cooled in transverse space for 1 s, then in momentum space for the following second. The reason for starting with betatron cooling is that the relatively high momentum spread (1.5%) provides a good randomization of the observations at each turn. In practice, some overlap between betatron and momentum cooling will certainly occur.

6.1 Betatron cooling

As the beam emittance is high and the cooling time is short ($\sim$ 1 s), the high-frequency system which is used for the cooling must have a broad bandwidth and a high power. If the gain of the system were to be optimum, the power would be equal to several hundreds of kilowatts in the 1-3 GHz frequency range. This is clearly out of the question. The power is in fact limited to a few kilowatts, and there is practically no heating due to the Schottky noise. The thermal noise is reduced to the lowest possible level by cooling pick-ups and preamplifiers at cryogenic temperatures. The cooling in this situation is well described during most of the time by the motion of the centre of gravity. At each turn, the centre of gravity observed at the distance a from the ideal orbit is displaced by a quantity Δa:

$$\Delta a = -ga \ ,$$

where g is the correction per turn. In the usual cooling systems g is constant and the emittance decreases exponentially, but after 1 s the cooling is insufficient. In our case, the product ga is kept constant by fitting the pick-up and kicker apertures to the beam size; the emittance decreases linearly and low emittances can be reached quickly (Fig. 14).

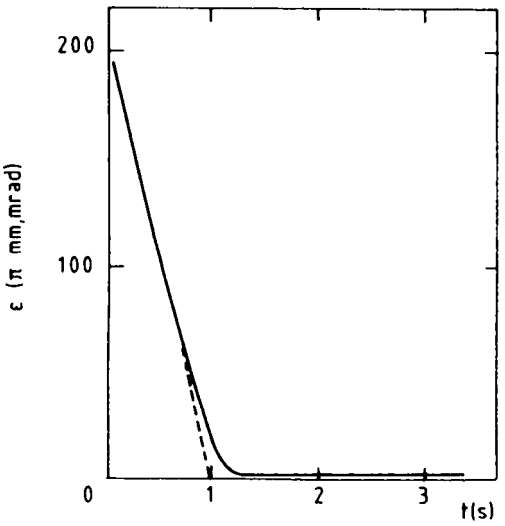

Fig. 14 Betatron cooling

The calculation of the betatron cooling parameters assumes broad band electrodes although the practical construction of the system will use the principle of 'stagger tuning' by dividing the whole frequency range into three sub-bands. In theory, emittances as low as 5 π mm·mrad can be reached. However, this mode of cooling has never been tested and, as a precaution, we have adopted the maximum emittance compatible with the accumulation (Section 7), 25 π mm·mrad, as a nominal value for the emittance at the end of the betatron cooling in the collector.

6.2 Momentum cooling

Since the betatron cooling is completed before the start of the Δp cooling, the movable electrodes are then near together so that they collect the full a.c. image current of the beam. It is to be noted that the same systems of detection and correction are used for both betatron and momentum cooling. The difference lies only in the signal processing. For the momentum cooling, the particle momentum spread is measured by observation of the dispersion of the revolution frequencies. The correction signal is processed in two cascaded filters (Fig. 15): the first one is passive and achieves the cooling by having notches at nominal revolution harmonics; the second one is active and has peaks at revolution harmonics to increase the loop gain around the notches.

By varying the electronic gain and working at constant power (2 kW), 85% of the particles are maintained in $2^{o}/_{oo}$ of the momentum spread after 1 s of cooling. Various parameters can

Fig. 15 Momentum cooling filters

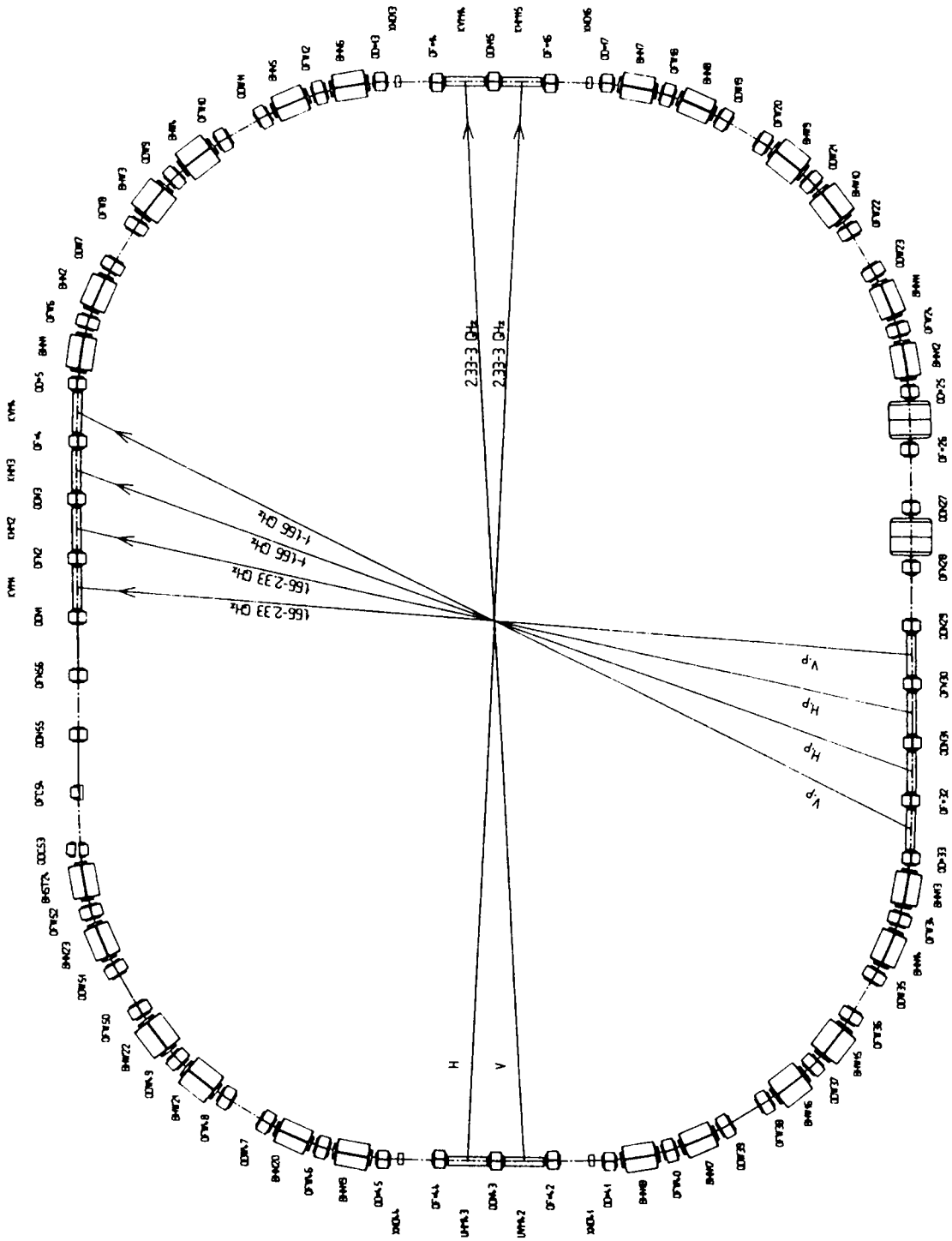

Fig. 16 The cooling systems in the ACOL lattice

be used to improve the momentum cooling, such as a dynamic change of the loop gain and the choice of the central momentum on an orbit of higher η ($\delta p/p = -2.25 \times 10^{-2}$ according to Fig. 8).

The complete layout of the collector with its cooling systems is shown in Fig. 16. As a recapitulation, the successive contractions of the beam during the debunching and cooling phases are plotted in Fig. 17.

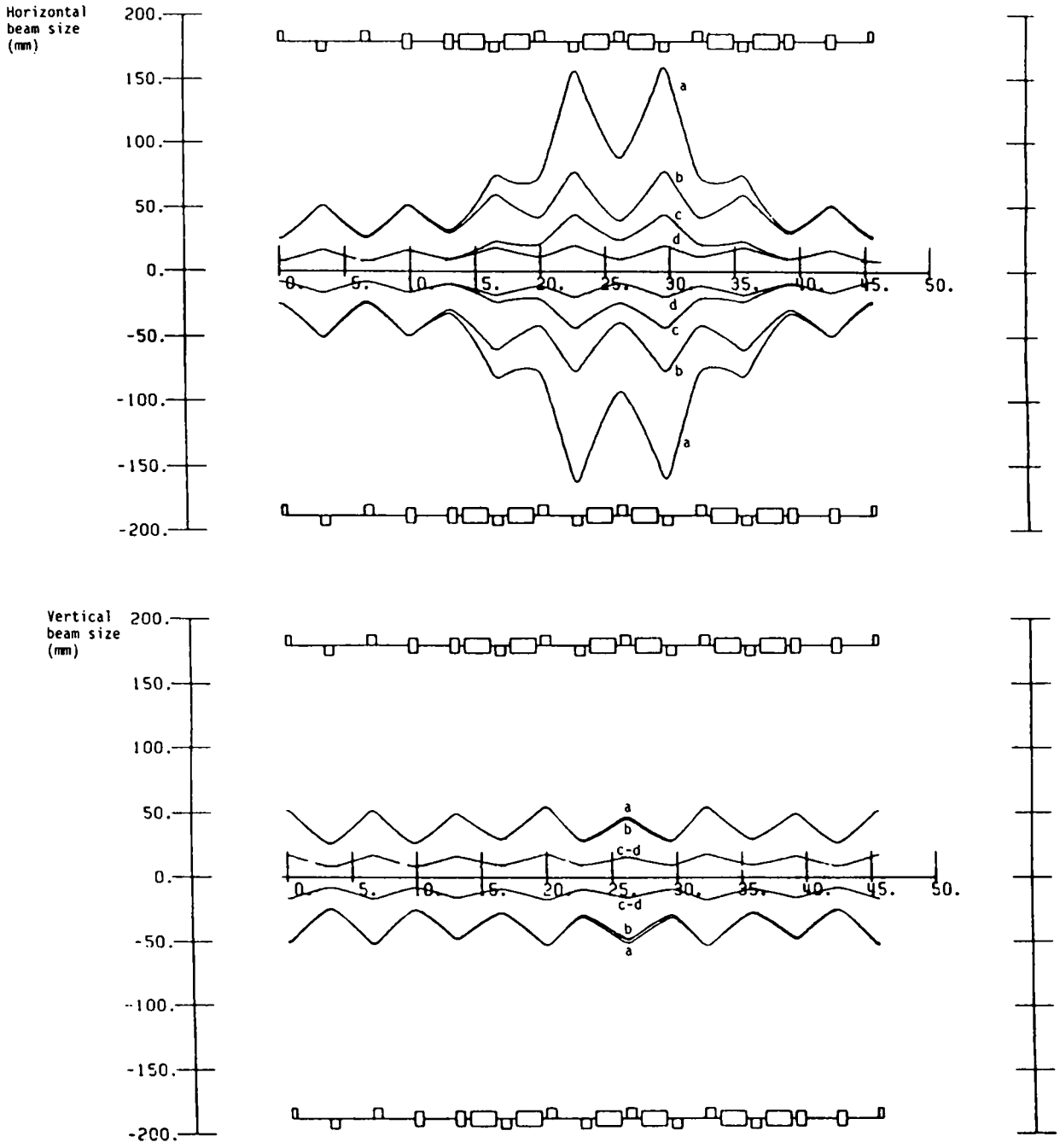

Fig. 17 Beam sizes at the different stages in ACOL
(a) after injection,
(b) after debunching,
(c) after betatron cooling,
(d) after momentum cooling.

7. ACCUMULATION

7.1 General description

The beam transfer from the collector to the accumulator is performed with the minimum dilution in phase-space density thanks to well-matched RF procedures of rebunching in the collector, capture and debunching in the accumulator, and well proven techniques of fast ejection and injection. In the precooling region of the AA, the full duration of a PS cycle is available and employed to perfect vertical and momentum cooling in the 1-2 GHz frequency range.

The most important changes will have to be made to the stochastic stacking systems. The new nominal accumulation rate (5×10^7 $\bar{p}$/pulse or 2.1×10^7 $\bar{p}$/s) is only a factor of 3 above the original AA design figure, but the new stacking system is designed for twice this rate, because experience has shown that achieving the theoretical cooling performance is often a long and arduous process.

This extra factor of 6 in stacking rate would be excluded without a considerable increase of bandwidth for both longitudinal cooling systems (stack tail and core). The transverse systems will be upgraded by extension of the bandwidth to 4-8 GHz and thus the transfer of antiprotons to SPS and LEAR will be less critical.

The stacking system presented here, and whose layout can be seen in Fig. 18, will use the frequency range 1-2 GHz for the stack tail system (i.e. 4 × the present frequencies),

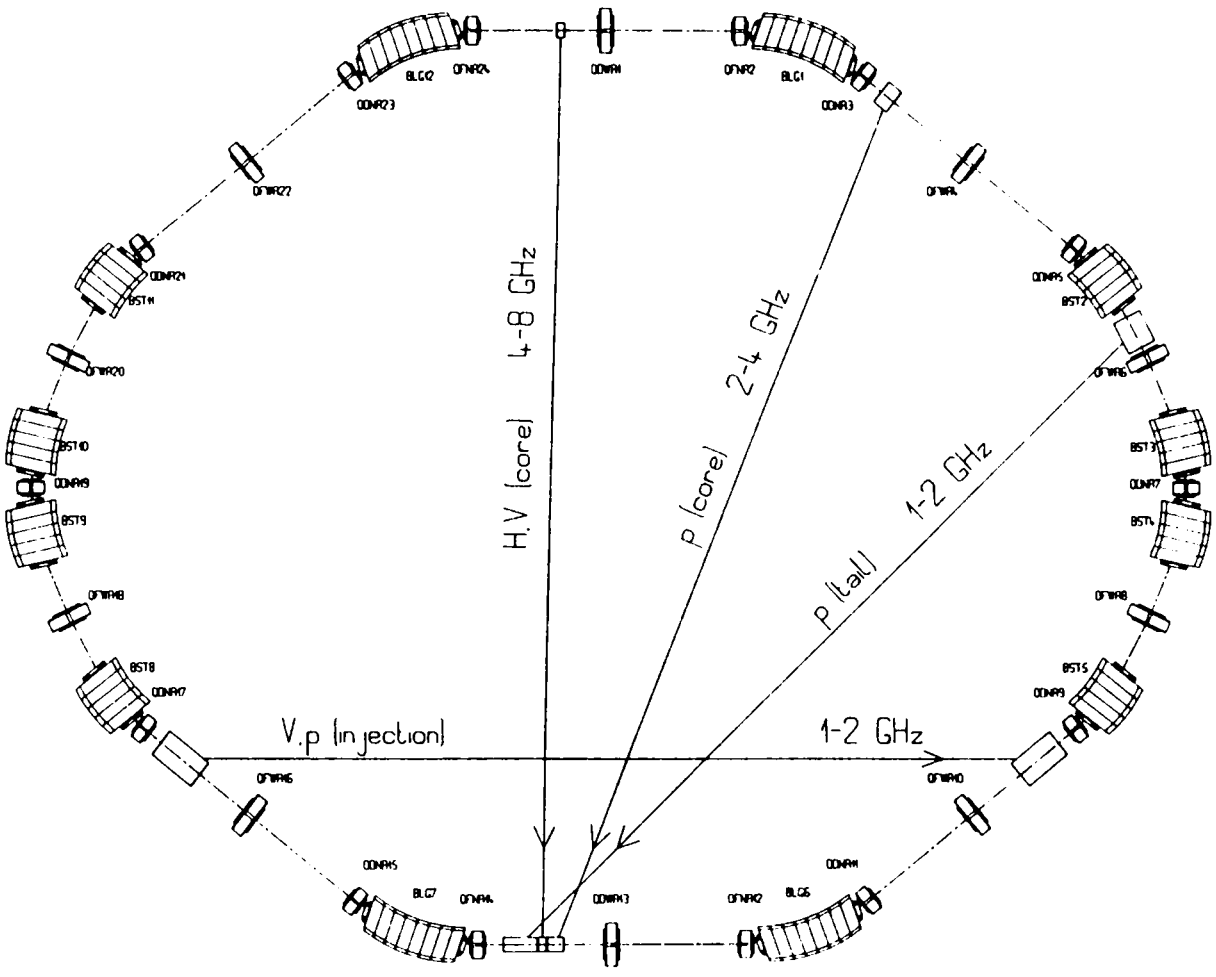

Fig. 18 The new stochastic systems in the Antiproton Accumulator

and 2-4 GHz for the core (twice the present values). This will allow us to double the final density so that the antiprotons may be extracted in 6 batches of 0.46 eV, holding 10^{11} particles each.

7.2 Stacking system design

The momentum spread of the stack will have to be reduced, both to keep the required wide-band power at a reasonable level and to avoid overlap of the Schottky bands at the higher frequencies. To reduce the influence of the stack tail system on the core particles, delay-line filters are proposed as in the present system, but modified for the higher frequency range. Investigation of a filterless system, using position-dependent kickers at a point with non-zero dispersion, has shown that this method (although promising some interesting simplifications) would not be feasible because the transverse kicks associated with such kickers and the transverse pick-up response would result in an open-loop gain of the system an order of magnitude above the longitudinal gain.

The reduced stack width will require the use of pick-ups with a steeper sensitivity profile versus beam position. This can only be achieved by reducing the vertical pick-up aperture. As a result, both the transverse dimensions and the momentum spread of the injected beam will have to be smaller than at present. In fact, the necessary performance of collector cooling is determined by what the AA stacking system can accept.

The exact requirements follow from lengthy numerical calculations, inevitable because of the large number of parameters that may be varied. As a result, the vertical and horizontal emittance should be less than 25 π mm·mrad and the final momentum spread in the collector should be about 0.2% (full width). The spread in the AA at deposit will be 1.16 times as high because of the circumference ratio.

Figure 19 shows a typical example of stack build-up, assuming that 10^8 particles per pulse are injected and stacked. The exact pulse-to-pulse behaviour at the deposit point still needs to be investigated; no problems are expected because of the large available aperture.

With the nominal stacking rate of 5×10^7 $\bar{p}$/pulse, the initial stack would be built up in 10 h; each successive fill would take 8 h. The maximum number of particles in the stack will be around 10^{12} as at present, limited by intra-beam scattering.

Here we are, or rather hope to be one day, at the top of the mountain!

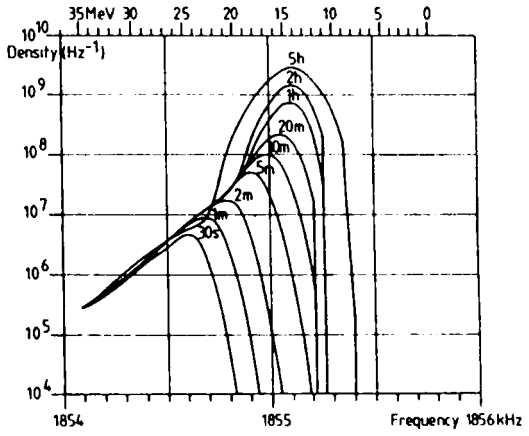

Fig. 19 Beam density profile in the AA

Acknowledgements

The working group which elaborated the design of the ACOL project was composed of: S.X. Fang and Z.Y. Guo (IHEP Beijing); B. Autin, O. Barbalat, M. Bell, R. Bellone, B. Bianchi, R. Billinge, G. Carron, V. Chohan, L. Coull, T. Dorenbos, D.C. Fiander, R. Garoby, W. Hardt, G. Himbury, K. Hollingworth, H. Horisberger, A. Ijspeert, C.D. Johnson, E. Jones, H. Koziol, F. Krienen, F. Malthouse, M. Martini, S. Maury, C. Metzger, K. Metzmacher, S. Milner, G. Nassibian, P. Pearce, F. Pedersen, B. Pincott, W. Pirkl, A. Poncet, K.H. Reich, H. Riege, L. Rinolfi, J.C. Schnuriger, T.R. Sherwood, P. Sievers, G. Stevenson, A.H. Sullivan, C. Taylor, L. Thorndahl, H.-H, Umstätter, W. van Cauter, S. van der Meer, F. Völker, B. Williams, E.J.N. Wilson and M. Zanolli (CERN); A. Wrülich (DESY); K. Frank and R. Seeböck (University of Erlangen); C. Hojvat (FNAL); M. Conte (University of Genoa); K. Preis and H. Stögner (IGTE Graz); G Wüsterfeld (KFA Jülich); L. de Menna, G. Miano and V. Vaccaro (University of Naples); P.H. Bruinsma (NIKHEF); J.R.J. Bennett, D.A. Gray, M. Harold and H.E. Jones (Rutherford Appleton Laboratory).

REFERENCES

1) Summary of the Antiproton Collector Study, AA-Longterm Note No. 26, December 1982.

2) S. van der Meer, Practical and foreseeable limitations in usable luminosity for the collider, Proc. Third Topical Workshop on Proton-Antiproton Collider Physics, Rome, January 1983, CERN 83-04 (1983), p. 555.

3) B. Autin, The future of the antiproton accumulator, *in* Antiproton physics and the W discovery, Proc. Third Moriond Workshop, La Plagne, Savoie, March 1983 (Ed. Frontières, Gif-sur-Yvette, 1983), p. 573.

4) G. Brianti, Experience with the CERN $p\bar{p}$ complex, IEEE Trans. Nucl. Sci. NS30, 1950 (1983).

5) B. Autin, Technical developments for an antiproton collector at CERN, Proc. 12th Int. Conf. on High-Energy Accelerators, Batavia, August 1983 (Fermilab, Batavia, 1984), p. 393.

6) Design study of an Antiproton Collector for the Antiproton Accumulator (ACOL), CERN 83-10 (1983).

7) Design report, Tevatron I project (Fermilab, Batavia, Illinois, 1983).

8) E. Jones, S. van der Meer, F. Rohner, J.C. Schnuriger and T.R. Sherwood, Antiproton production and collection for the CERN Antiproton Accumulator, IEEE Trans. Nucl. Sci., NS30, 2778 (1983).